Source of Acquisition
CASI Acquired

SECRET

CLASSIFICATION CANCELLED

Copy #

RM SA54H26b

NACA RM SA54H26b

OCT 7

NACA

CLASSIFICATION CANCELLED
Authority NASA PUBLICATIONS
ANNOUNCEMENTS NO. 13
Date By

Restriction/Classification Cancelled

RESEARCH MEMORANDUM

for the

United States Air Force

WIND-TUNNEL INVESTIGATION AT SUBSONIC AND SUPERSONIC SPEEDS OF A
FIGHTER MODEL EMPLOYING A LOW-ASPECT-RATIO UNSWEPT WING
AND A HORIZONTAL TAIL MOUNTED WELL ABOVE THE WING
PLANE - LATERAL AND DIRECTIONAL STABILITY

By Benton E. Wetzel

Ames Aeronautical Laboratory
Moffett Field, Calif.

CLASSIFICATION CHANGED TO
Restriction/Classification Cancelled

CONFIDENTIAL

NACA change # 2864

Restriction/Classification Cancelled

This material contains information affecting the National Defense of the United States within the meaning
of the espionage laws, Title 18, U.S.C., Secs. 793 and 794, the transmission or revelation of which in any
manner to an unauthorized person is prohibited by law.

NATIONAL ADVISORY COMMITTEE
FOR AERONAUTICS
WASHINGTON
August 26, 1954

CLASSIFICATION CANCELLED

FILE COPY
To be returned to
the files of the National
Advisory Committee
for Aeronautics
Washington, D.C.

60 RDZ 4007

CLASSIFICATION CANCELLED

Authority NASA PUBLICATIONS
ANNOUNCEMENTS NO.
Date ___ By ___

NATIONAL ADVISORY COMMITTEE FOR AERONAUTICS

RESEARCH MEMORANDUM

for the

United States Air Force

WIND-TUNNEL INVESTIGATION AT SUBSONIC AND SUPERSONIC SPEEDS OF A
FIGHTER MODEL EMPLOYING A LOW-ASPECT-RATIO UNSWEPT WING
AND A HORIZONTAL TAIL MOUNTED WELL ABOVE THE WING
PLANE - LATERAL AND DIRECTIONAL STABILITY

By Benton E. Wetzel

SUMMARY

The static lateral- and directional-stability characteristics of a
high-speed fighter-type airplane, obtained from wind-tunnel tests of a
model, are presented. The model consisted of a thin, unswept wing of
aspect ratio 2.5 and taper ratio 0.385, a body, and a horizontal tail
mounted in a high position on a vertical tail. Rolling-moment, yawing-
moment, and cross-wind-force coefficients are presented for a range of
sideslip angles of -5° to +5°, for Mach numbers of 0.90, 1.45, and 1.90.

Data are presented which show the effects on the lateral and direc-
tional stability of: (1) component parts of the complete model, (2) mod-
ification of the empennage so as to provide different heights of the
horizontal tail above the wing plane, (3) angle of attack, and (4) dihe-
dral of the wing.

INTRODUCTION

A model of a high-speed fighter airplane has been the subject of an
investigation at subsonic and supersonic speeds in the Ames 6- by 6-foot
supersonic wind tunnel. The model is representative of current designs
for airplanes with unswept-wing plan forms and with horizontal tails
mounted well above the wing-chord plane. In order to determine which
design arrangements offer promise from the standpoint of static longitu-
dinal and directional stability, various combinations of the model com-
ponents have been tested. The results of these tests provide information
regarding the effect of mutual interference on the contributions of the
components to the stability of the complete model.

SECRET

60 RDZ 4007

This report presents the results of the lateral and directional investigation of that model, and is a companion paper to an earlier research memorandum (ref. 1) which was concerned with the longitudinal-stability characteristics of the model. The primary purposes of this paper are to point out some of the important interference effects, especially those between the horizontal- and vertical-tail surfaces, and to show their contributions to the static lateral and directional stability.

NOTATION

All force coefficients presented herein are referred to the wind axes; all moment coefficients to the stability axes. The moment center was placed at the projection of the 25-percent mean aerodynamic chord point on the longitudinal axis of the body.

The following notation has been used in this report:

b model wing span, in.

C_l rolling-moment coefficient, $\dfrac{\text{rolling moment}}{qSb}$

C_n yawing-moment coefficient, $\dfrac{\text{yawing moment}}{qSb}$

C_Y cross-wind-force coefficient, $\dfrac{\text{cross-wind force}}{qS}$

c local chord of the wing, in.

$\bar{c}$ mean aerodynamic chord of the wing, $\dfrac{\int_0^{b/2} c^2 dy}{\int_0^{b/2} c \, dy}$, in.

h height of the horizontal tail above the body axis, in.

l_t horizontal-tail length, measured between the 25-percent mean aerodynamic chord stations of the wing and the horizontal tail, in.

l_v vertical-tail length, measured between the 25-percent mean aerodynamic chord stations of the wing and the vertical tail, in.

M free-stream Mach number

q free-stream dynamic pressure, lb/sq in.

R Reynolds number, based on the mean aerodynamic chord

S   model wing area, formed by extending the leading and trailing
         edges to the plane of symmetry, sq in.

S_V area of vertical tail, including portion enclosed in body by
         extending leading edge to body axis, sq in.

y   spanwise distance from plane of symmetry, in.

α angle of attack of the body, deg

β angle of sideslip, deg

Γ angle of wing dihedral, deg

       In addition, the following notation has been used in order to denote
various components of the model:

B   body

H_1 horizontal tail, when located 7.13 inches above the body axis

H_2 horizontal tail, when located 8.15 inches above the body axis

V_1 vertical tail used with horizontal tail H_1

V_2 vertical tail used with horizontal tail H_2

W   wing

APPARATUS AND MODEL

       The experimental investigation was performed in the Ames 6- by 6-foot
supersonic wind tunnel. This wind tunnel, which has a closed section
and is of the variable-pressure type, is operated at Mach numbers varying
from 0.60 to 0.90 and from 1.20 to 1.90. A complete description of the
wind tunnel and the characteristics of the air stream at supersonic speeds
can be found in reference 2. In this wind tunnel, models are sting-mounted
and the forces on the models are measured with internal electrical strain-
gage balances. The balance used for the present tests was of the flexure-
pivot type. A photograph of the model mounted in the wind tunnel is shown
in figure 1.

       The complete model consisted of an unswept wing of aspect ratio 2.5,
a horizontal tail mounted in a high position on a vertical tail, and a
body with a circular cross section modified by the addition of a canopy
and protuberances simulating side inlets. A dimensional sketch of the

model and its parts is shown in figure 2, and a compilation of the geo-
metric characteristics is presented in table I. The model was designed
to permit tests of the wing and body as a unit and in combination with
various components of the empennage. Two different vertical tails were
built, which allowed mounting the horizontal tail in two different posi-
tions above the plane of the wing. All parts of the model were made of
steel, with the exception of the body, which was constructed of aluminum.

TESTS AND PROCEDURES

Range of Test Variables

Rolling moment, yawing moment, and cross-wind force were measured
throughout a range of sideslip angles varying from -5° to +5° at Mach
numbers of 0.90, 1.45, and 1.90, at a Reynolds number of 2.4 million.
Although most of the tests were performed at zero angle of attack, some
data were obtained at an angle of attack of 5°. Tests were made of a
number of combinations of the components of the model. The various com-
binations and test conditions are enumerated in table II.

Reduction of Data

Data presented herein have been reduced to NACA coefficient form.
The reader is referred to the section on notation for complete descriptions
of the coefficients used. It should be noted that the cross-wind-force
coefficient is referred to the wind axes, while the rolling- and yawing-
moment coefficients are referred to the stability axes.

Corrections have been made to the data to account for differences
known to exist between measurements made in the wind tunnel and in a
free-air stream. Corrections made to the data presented herein account
for the following factors:

1. The increase in airspeed in the vicinity of the model at subsonic
   speed as a result of constriction of the air stream by the
   walls of the wind tunnel.

2. The change in angle of attack of the model induced by the walls
   of the wind tunnel at subsonic speeds as a consequence of the
   lift on the model. The correction amounted to: $\Delta\alpha = 0.315 \, C_L$.

It should be pointed out that, for the lateral tests, the model was
mounted in the wind tunnel with the wing horizontal. As a result, non-
uniformities of the air stream had a greater effect on the data presented
in this report than on those of reference 1. The reader's attention is

directed to reference 2, wherein he will find detailed information about
the characteristics of the air stream at supersonic speeds.

RESULTS AND DISCUSSION

Results are presented herein which show the effects of the following
on the lateral and directional stability:

1. Various components of the complete model

2. Modification of the empennage so as to provide different heights
   of the horizontal tail above the wing plane

3. Angle of attack

4. Dihedral of the wing

Although all of these results will be discussed, the primary purpose
of this report is to discuss some of the important effects of interference
between component parts on the lateral-. and directional-stability char-
acteristics of the complete model. The interferences discussed are some
of those which affect the contributions of the tail surfaces to the sta-
bility and not those which affect the contributions of the wing and body.
Although the tests performed did not allow a complete quantitative sepa-
ration of these interference effects, they did provide an instructive
qualitative study.

Effects of Model Components

The effects of various components of the model on the variation with
sideslip angle of the rolling-moment, yawing-moment, and cross-wind-force
coefficients are shown in figure 3. The wing-body combination was unstable
both laterally and directionally. When the vertical tail was added to the
wing-body model, the large cross-wind force carried by the vertical tail
resulted in rolling- and yawing-moment contributions large enough to pro-
vide lateral and directional stability.

With the addition of the horizontal tail, the model was provided with
additional lateral and directional stability, as a result of two effects
arising from the mutual interference between the horizontal- and vertical-
tail surfaces. Consider, first, the effect of the addition of the hori-
zontal tail on the characteristics of the vertical tail. This, the so-
called end-plate effect of the horizontal tail in increasing the effective
aspect ratio of the vertical tail, resulted in an increased rate of change
of cross-wind force with sideslip angle at a Mach number of 0.90. This
effect increased both the lateral and the directional stability at that

Mach number. At supersonic speed, the influence of the horizontal tail
decreased with increasing Mach number since the influence of the tail
was confined within the Mach cone from the tip of the vertical tail.

The second interference effect, that of the vertical tail on the
characteristics of the horizontal tail, occurred at both subsonic and
supersonic speeds. Because the horizontal tail was located near the
tip of the vertical tail, only its lower surface was influenced by the
loading on the vertical tail. The pressure differential between the two
surfaces of the vertical tail induced an asymmetric loading on the hori-
zontal tail which resulted in additional lateral stability for the complete
model.

Effect of Modifying Empennage

The effect on the lateral and directional stability of modifying
the empennage so as to mount the horizontal tail in a higher position
above the wing plane is shown in figure 4. The results showed that the
model with the higher horizontal tail was more stable both laterally and
directionally. Although a first appraisal of these data might indicate
a significant effect of horizontal-tail height, analysis of the data
indicated that most of the increased stability could be accounted for
by the larger span and greater aspect ratio of the vertical tail used with
the higher horizontal tail. Since the nondimensional tail height (the
ratio of horizontal-tail height h to vertical-tail span) was not sig-
nificantly different for the two empennages, no difference in the end-
plate effect at subsonic speeds should be expected.

Effect of Angle of Attack

The effect of angle of attack on the lateral and directional stability
of the wing-body and the wing-body-tail combinations is presented in
figure 5. As in the case at zero angle of attack, the wing-body combina-
tion was unstable both laterally and directionally at an angle of attack
of 5°. The lateral instability was, of course, decreased when the model
was tested at $\alpha = 5°$.

The lateral and directional stability of the complete model increased
as angle of attack increased except at M = 1.90, where this effect was
reversed. The increase in directional stability at M = 0.90 and M = 1.45
resulted from an increase in cross-wind force carried by the vertical
tail, believed attributable to the sidewash component of the vorticity
discharged from the wing. At M = 1.90, however, the vertical tail lies
outside the Mach cones from the wing tips but within the region bounded
by the waves from the leading and trailing edges of the wing. Since the
vertical tail was no longer influenced by the vorticity from the wing

tips but was primarily influenced by the flow field above the wing, it is not surprising that the cross-wind force and the attendant rolling and yawing moments produced by the tail were reduced.

Effect of Dihedral

The effect of variation of wing dihedral is presented in figure 6 for the wing-body and wing-body-tail combinations. As would be expected, variation of dihedral affected primarily the lateral stability of the models. The variation of wing dihedral caused only small differences in the contributions of the tail surfaces to the lateral and directional stability of the complete model.

CONCLUDING REMARKS

Wind-tunnel studies of a model of a fighter airplane with an unswept wing showed that mutual interference between the vertical- and horizontal-tail surfaces played a significant role in the contribution of the empennage to the stability of the complete airplane. The horizontal tail, mounted near the tip of the vertical tail, acted as an end plate and increased the loading on the vertical tail, resulting in an increase in the contribution of the vertical tail to both the lateral and directional stability at a Mach number of 0.90. The presence of the vertical tail resulted in an asymmetric loading on the horizontal tail which provided a small amount of additional lateral stability at both subsonic and supersonic speeds.

Ames Aeronautical Laboratory
       National Advisory Committee for Aeronautics
              Moffett Field, Calif., Aug. 26, 1954.

                                        Benton E. Wetzel
                                        Benton E. Wetzel
                                   Aeronautical Research Scientist

Approved: *Victor J. Stevens*
                    H. Julian Allen
          Chief, High-Speed Research Division

REFERENCES

1. Smith, Willard G.: Wind-Tunnel Investigation at Subsonic and Super-
    sonic Speeds of a Fighter Model Employing a Low-Aspect-Ratio Unswept
    Wing and a Horizontal Tail Mounted Well Above the Wing Plane -
    Longitudinal Stability and Control. NACA RM A54D05, 1954.

2. Frick, Charles W., and Olson, Robert N.: Flow Studies in the Asym-
    metric Adjustable Nozzle of the Ames 6- by 6-Foot Supersonic Wind
    Tunnel. NACA RM A9E24, 1949.

TABLE I.- GEOMETRIC CHARACTERISTICS OF THE MODEL

Wing
  Aspect ratio 2.50
  Taper ratio 0.385
  Airfoil section (streamwise) . . . Modified biconvex with elliptical
                                                          leading edge
    Thickness-chord ratio, percent chord 3.4
  Area, S, sq in. 202.50
  Chord at plane of symmetry, in. 13.00
  Chord at tip, in. 5.00
  Mean aerodynamic chord, in. 9.59
  Span 22.50
  Dihedral, deg . . . . -5 or -10
  Incidence, deg   0
  Sweep of leading edge, deg 27.1
Body
  Length, in. 45.39
Vertical tail, V_1
  Stabilizer
    Aspect ratio 1.07
    Airfoil section (parallel to body axis) . . . . . Modified biconvex
                                                  with sharp leading edge
      Thickness-chord ratio for section 2.32 in. above
        body axis, percent chord 4.25
      Thickness-chord ratio for section 7.13 in. above
        body axis, percent chord 5.00
    Area, S_V, including portion enclosed in body by
      extending leading edge to body axis, sq in. 59.51
    Chord of airfoil section 2.32 in. above body axis, in. . . . 9.65
    Chord of airfoil section 7.13 in. above body axis, in. . . . 4.46
    Mean aerodynamic chord, in. 7.93
    Span, in. 7.98
    Tail length, l_V, in. 12.93
    Tail volume, $\dfrac{l_V}{b} \dfrac{S_V}{S}$ 0.1689
    Sweep of leading edge, deg 44
  Dorsal fin
    Area, exposed, sq in. 2.17
  Total exposed area, stabilizer and dorsal fin, sq in. 44.64
Vertical tail, V_2
  Stabilizer
    Aspect ratio 1.26
    Airfoil section (parallel to body axis) . . . . . Modified biconvex
                                                with elliptical leading edge
      Thickness-chord ratio for section 2.32 in. above
        body axis, percent chord 4.5

TABLE I.- GEOMETRIC CHARACTERISTICS OF THE MODEL - Concluded

```
    Thickness-chord ratio for section 8.15 in. above
        body axis, percent chord . . . . . . . . . . . . . . . . 5.25
    Area, S_v, including portion enclosed in body by
        extending leading edge to body axis, sq in. . . . . . . . 60.60
    Chord of airfoil section 2.32 in. above body axis, in.  . . .9.18
    Chord of airfoil section 8.15 in. above body axis, in. . . . 4.12
    Mean aerodynamic chord, in. . . . . . . . . . . . . . . . . . 7.35
    Span, in. . . . . . . . . . . . . . . . . . . . . . . . . . . 8.75
    Tail length, l_v, in.  . . . . . . . . . . . . . . . . . . . 13.24
                    l_v S_v
    Tail volume,    --- ---  . . . . . . . . . . . . . . . . . . 0.1761
                    b   S
    Sweep of leading edge, deg . . . . . . . . . . . . . . . . . . 38
Dorsal fin
    Area, exposed, sq in. . . . . . . . . . . . . . . . . . . . . 2.38
Total exposed area, stabilizer and dorsal fin, sq in. . . . . 44.88
Horizontal tail (both H_1 and H_2)
Aspect ratio . . . . . . . . . . . . . . . . . . . . . . . . . . 2.89
Taper ratio . . . . . . . . . . . . . . . . . . . . . . . . . . 0.326
Airfoil section (streamwise) . . . Modified biconvex with elliptical
                                                    leading edge
    Thickness-chord ratio at plane of symmetry, percent chord . . . 5
    Thickness-chord ratio at tip, percent chord . . . . . . . . . . 3
Area, sq in. . . . . . . . . . . . . . . . . . . . . . . . . . 49.80
Chord at plane of symmetry, in. . . . . . . . . . . . . . . . . 6.26
Chord at tip, in. . . . . . . . . . . . . . . . . . . . . . . . 2.04
Mean aerodynamic chord, in. . . . . . . . . . . . . . . . . . . 4.51
Span, in. . . . . . . . . . . . . . . . . . . . . . . . . . . 12.00
Tail length, l_t, in. . . . . . . . . . . . . . . . . . . . . 17.22
Dihedral, deg . . . . . . . . . . . . . . . . . . . . . . . . . . 0
Incidence, deg . . . . . . . . . . . . . . . . . . . . . . . . . 0
Sweep of 50-percent-chord line, deg . . . . . . . . . . . . . . . 0
```

TABLE II.- MODEL COMBINATIONS AND TEST CONDITIONS

Model	Γ, deg	α, deg	Figure no.
WB	-5	0	6
	-10	0	3, 5, 6
	-10	5	5
WBV$_1$	-10	0	3
WBV$_1$H$_1$	-10	0	3, 4, 5
	-10	5	5
WBV$_2$H$_2$	-5	0	6
	-10	0	4, 6
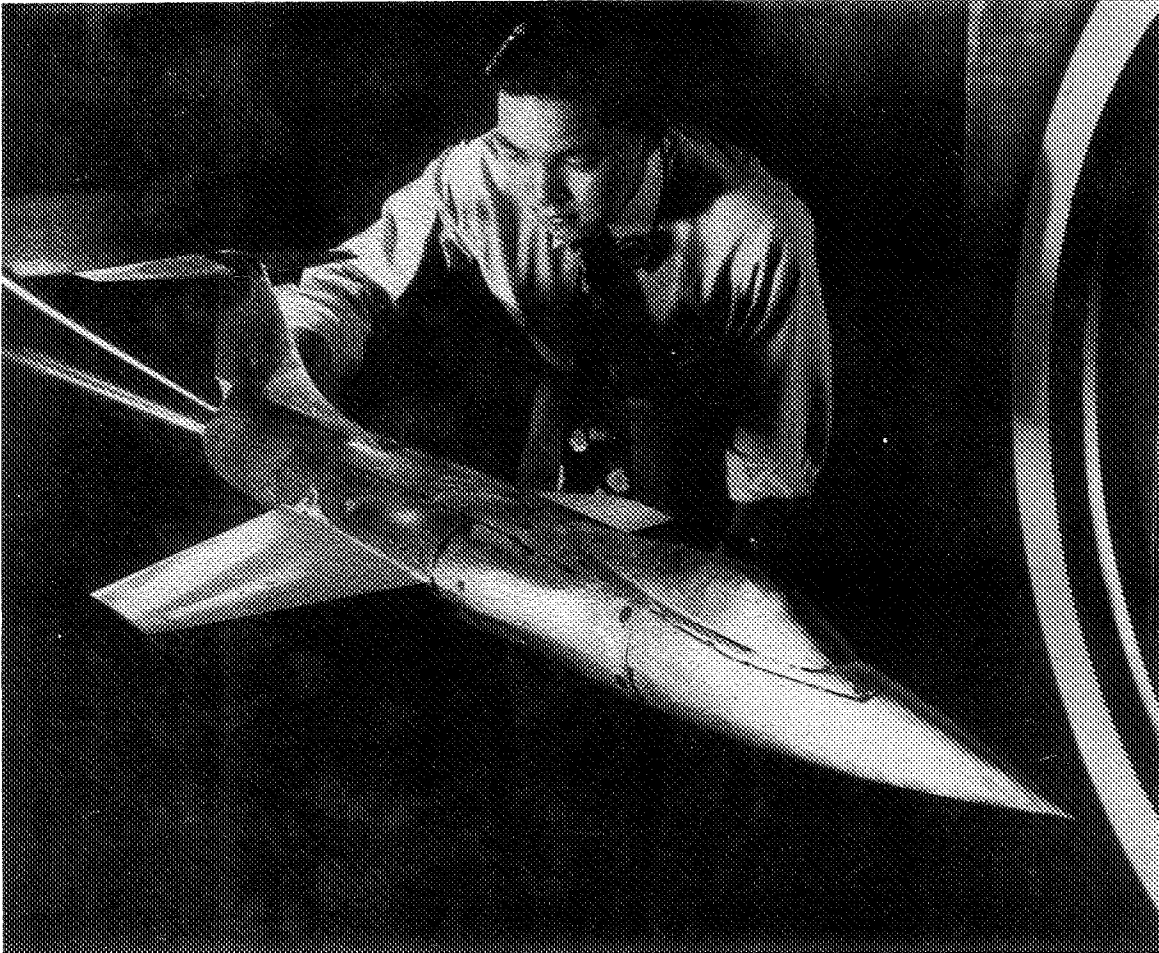
A-18101.1

Figure 1.- Three-quarter front view of fighter model in the Ames 6- by 6-foot supersonic wind tunnel.
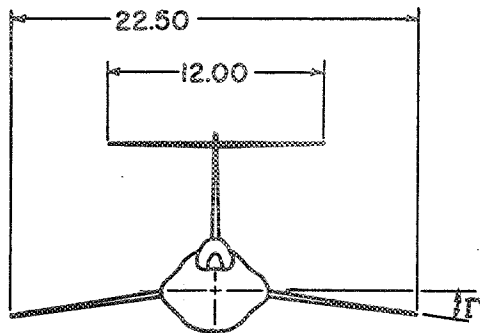
Models tested with $\Gamma = -5°$ and $-10°$

Moment center at 25% $\bar{c}$

See fig. 2(b)
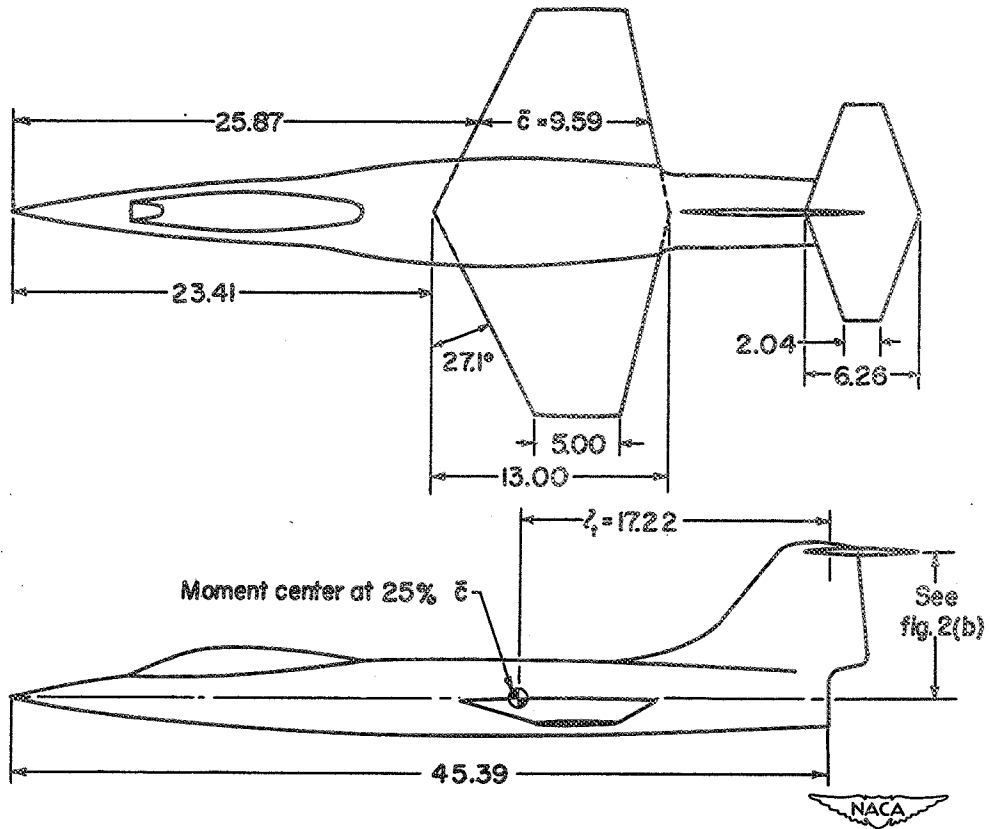
All dimensions shown in inches unless otherwise noted.

(a) Three-view sketch of model.

Figure 2.- Dimensional sketches of models.

Empennage V_1 H_1
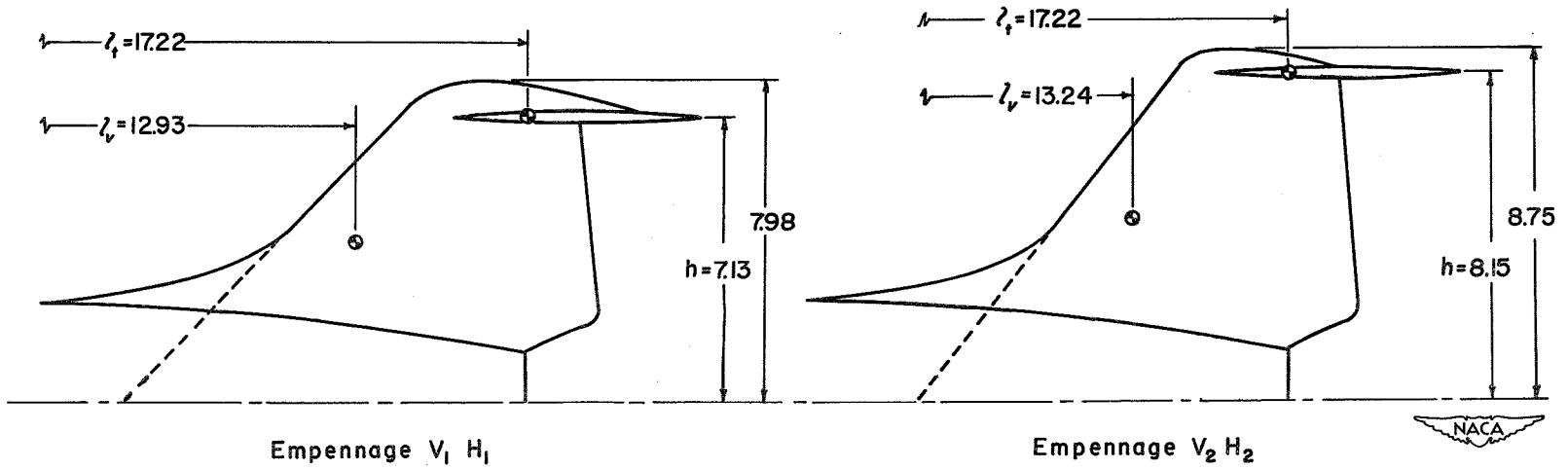
Empennage V_2 H_2

(b) Empennages tested.

Figure 2.- Concluded.
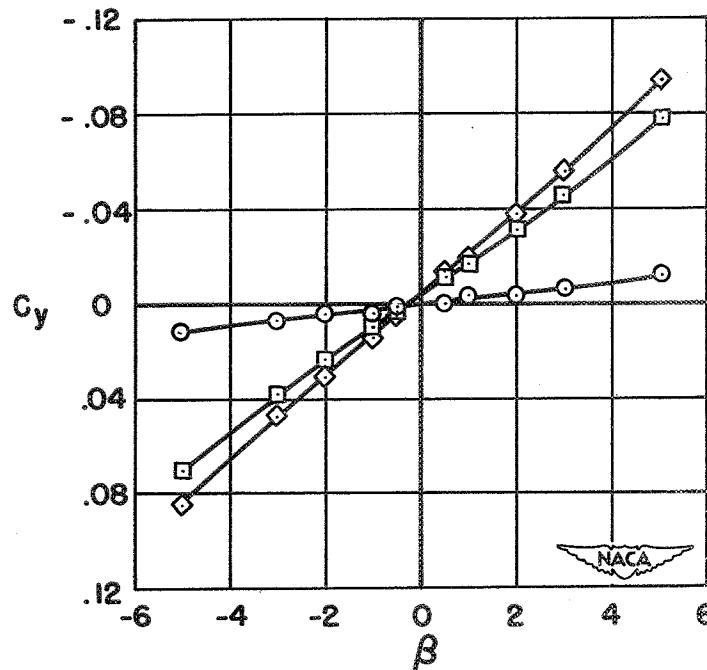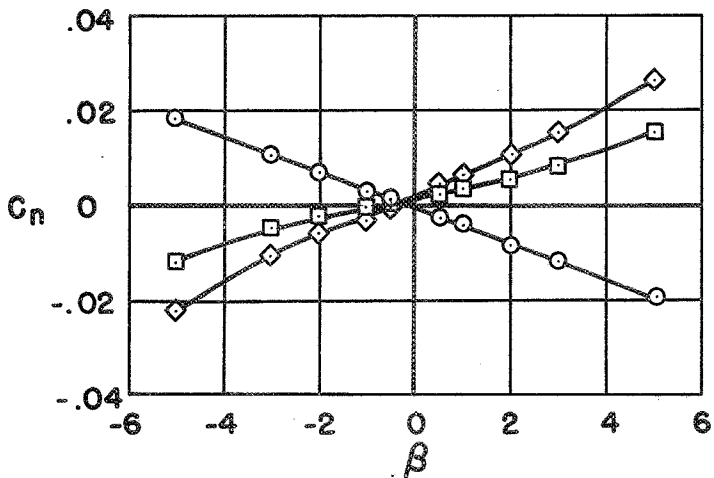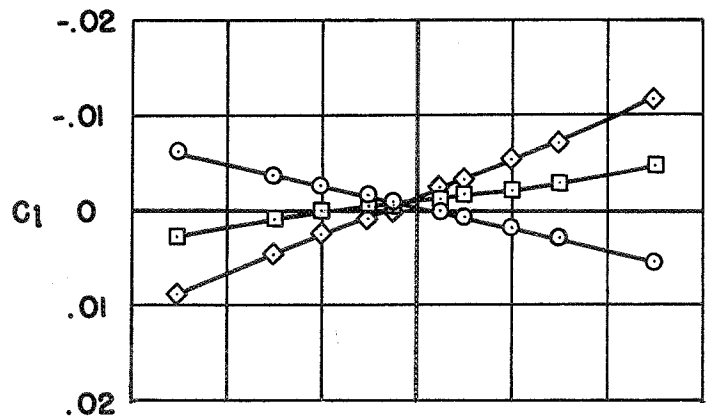
(a) M = 0.90

Figure 3.- Effect of model components on the variation with sideslip angle of the rolling-moment, yawing-moment, and cross-wind-force coefficients for a model of a fighter airplane; $\Gamma = -10°$; $\alpha \approx 0°$.

○ Less empennage

□ Less horizontal tail

◇ Complete ; h = 7.13 in.
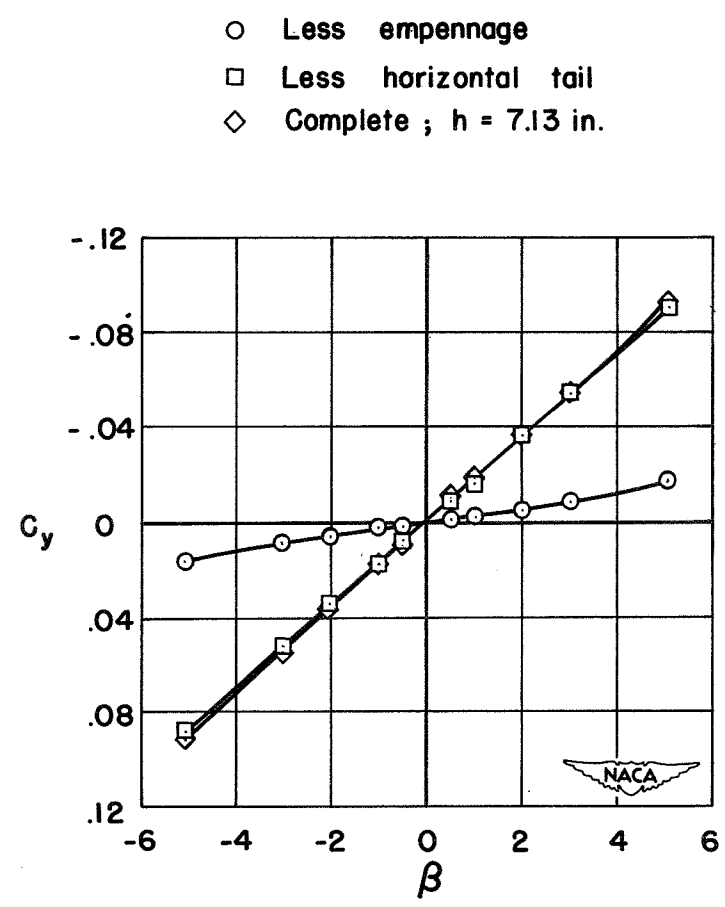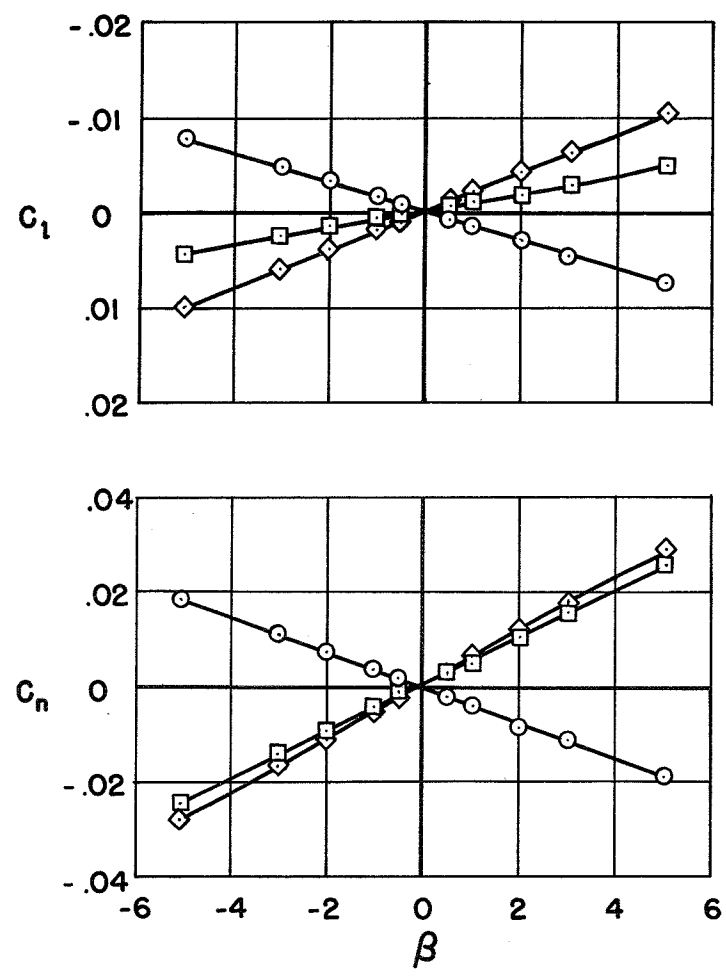
(b) M = 1.45

Figure 3.- Continued.

o   Less   empennage

□   Less   horizontal   tail

◇   Complete ; h = 7.13 in.
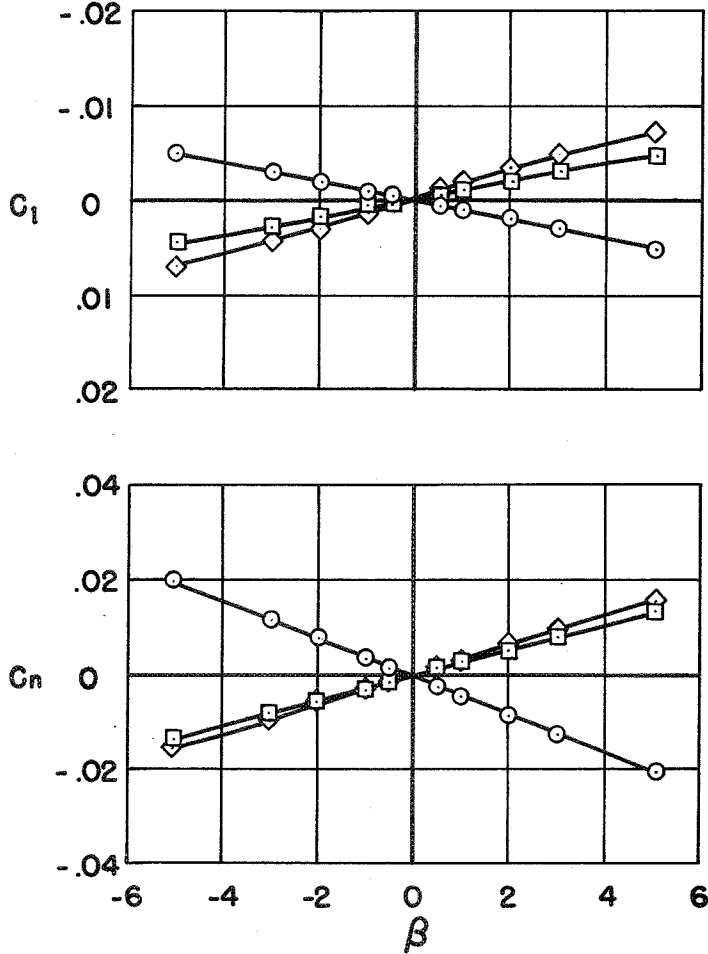
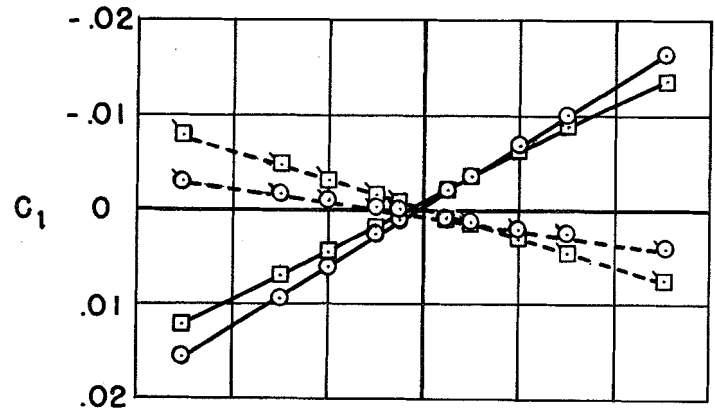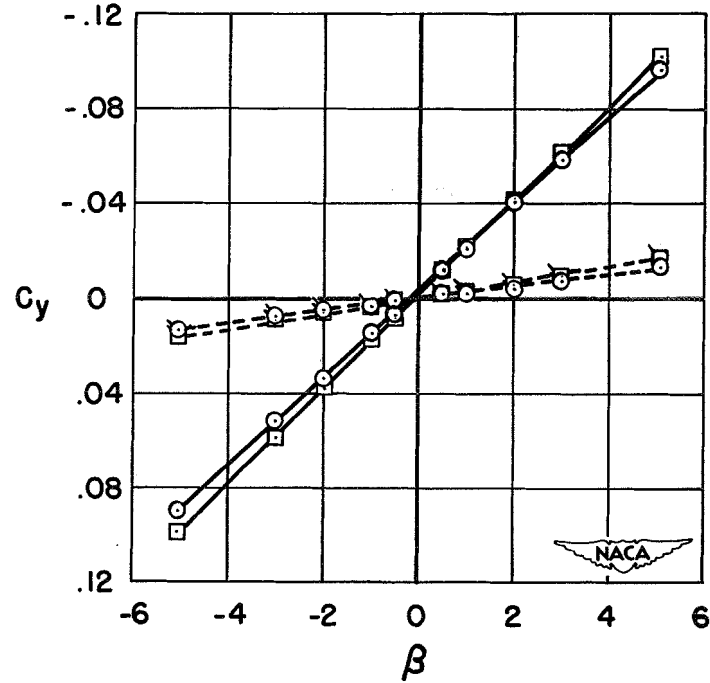(c) M = 1.90

Figure 3.- Concluded.
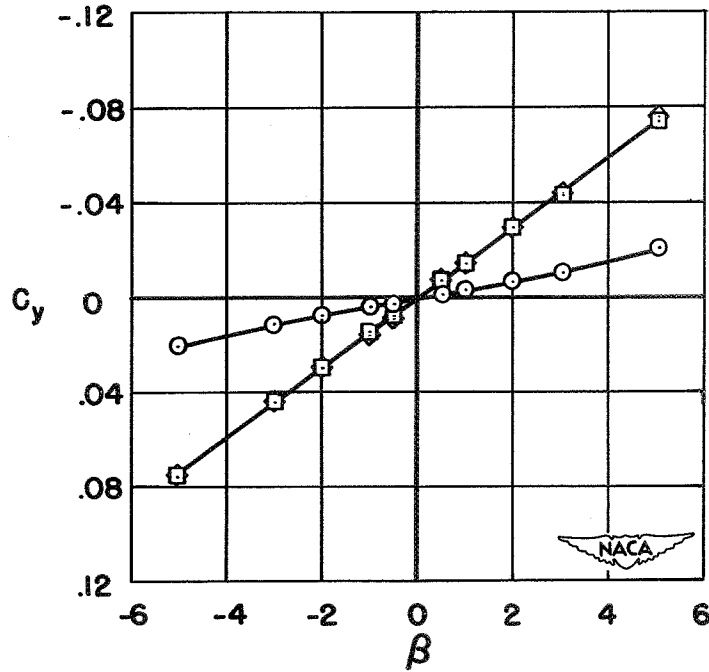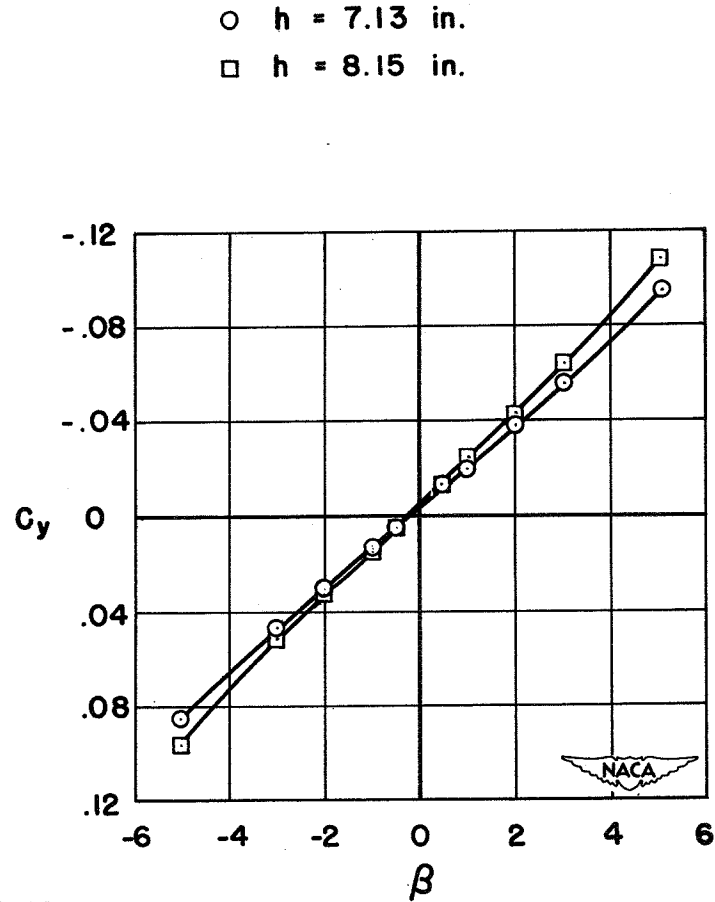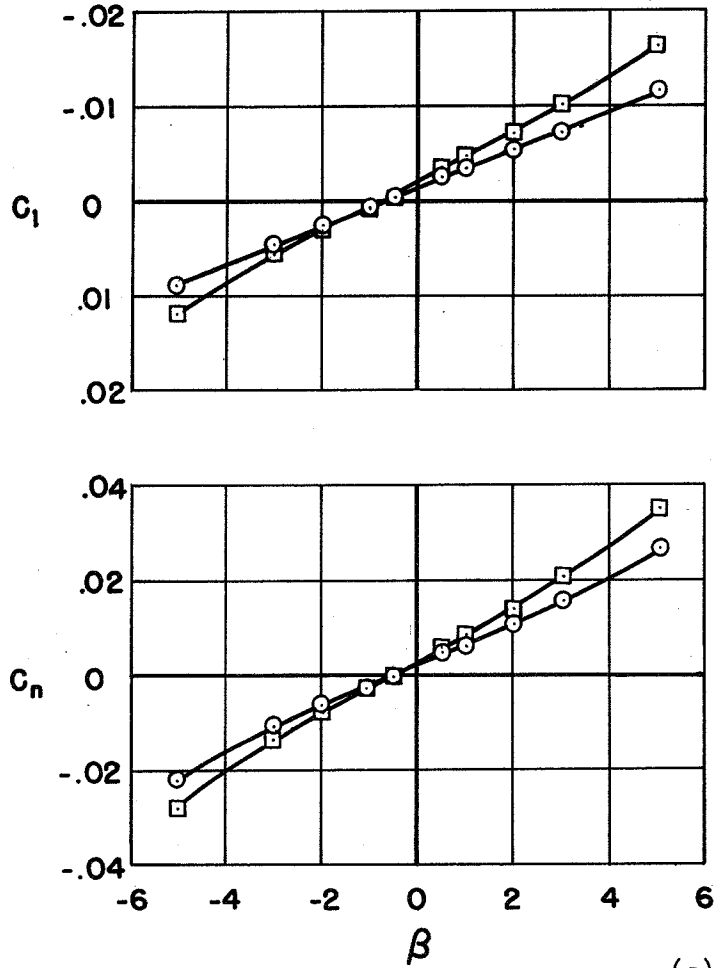
(a) M = 0.90

Figure 4.- Effect of modifying the empennage on the variation with sideslip angle of the rolling-moment, yawing moment, and cross-wind-force coefficients for a model of a fighter airplane; $\Gamma = -10°$, $\alpha \approx 0°$.
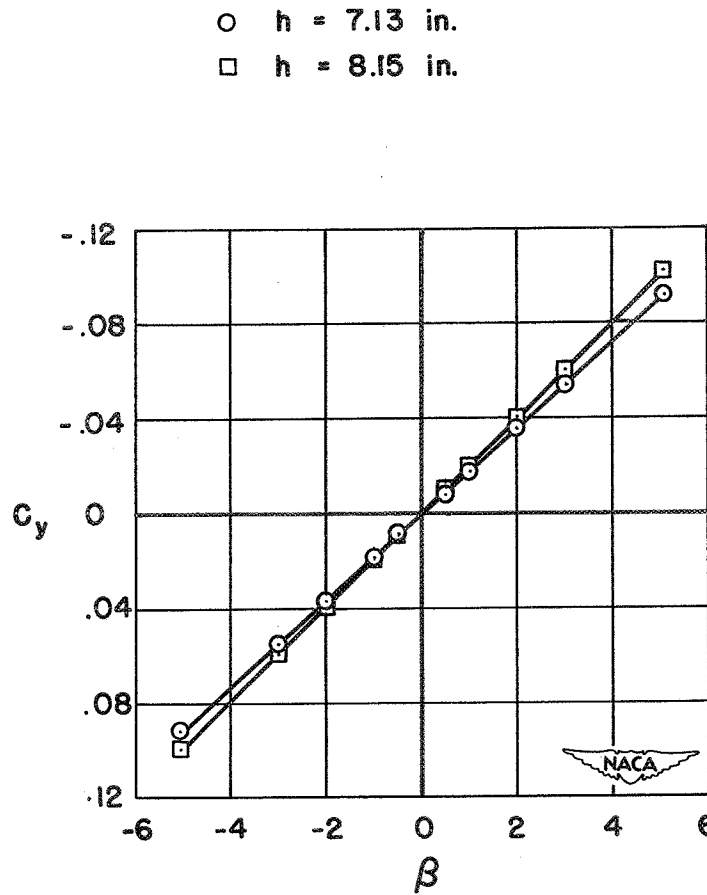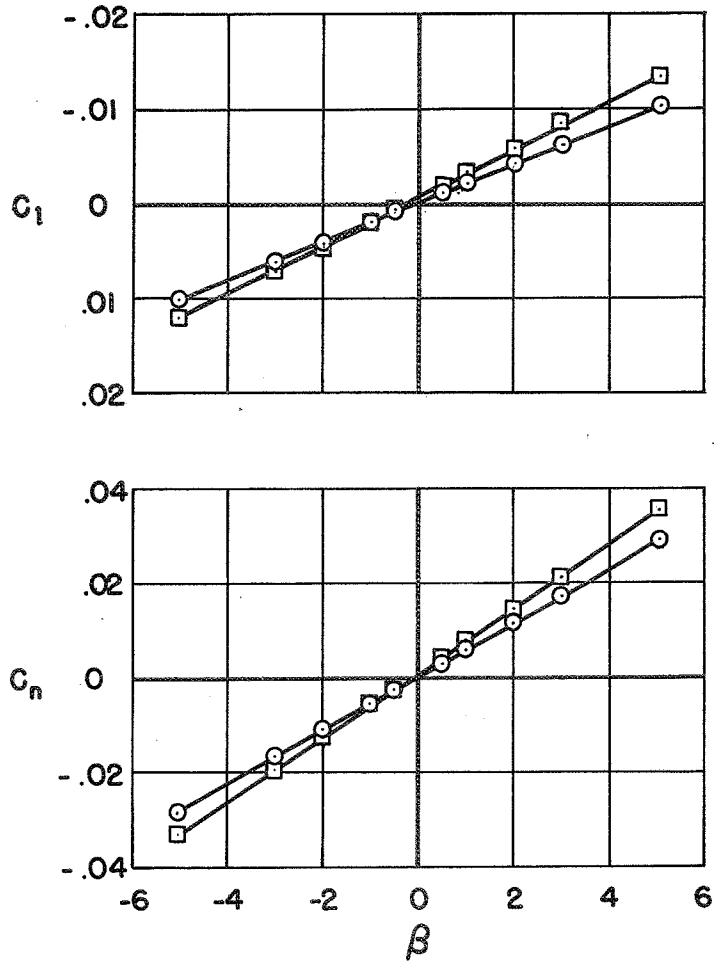
(b) M = 1.45

Figure 4.- Continued.

○   h = 7.13   in.
□   h = 8.15   in.
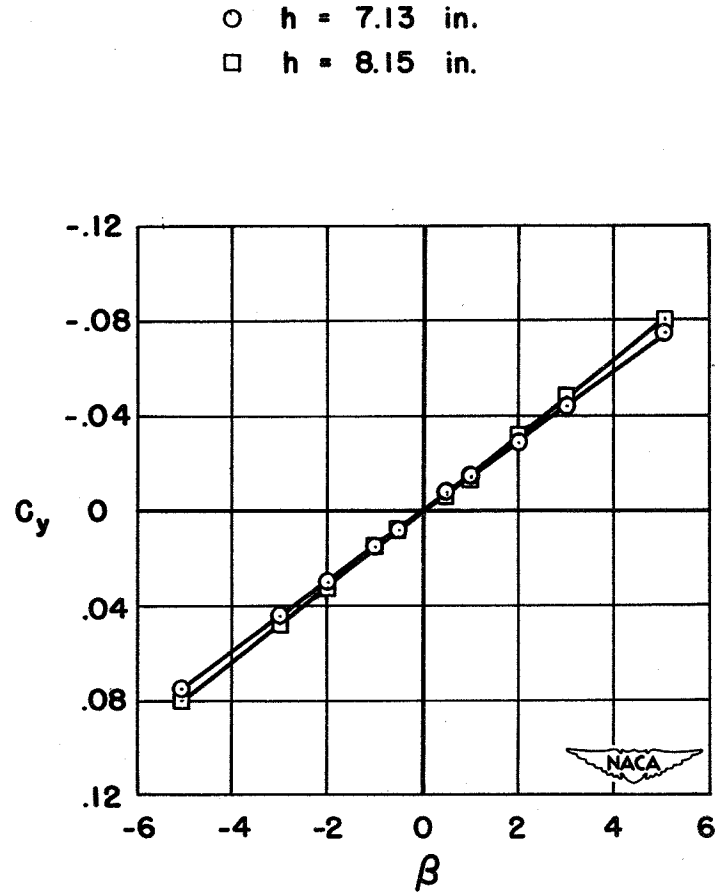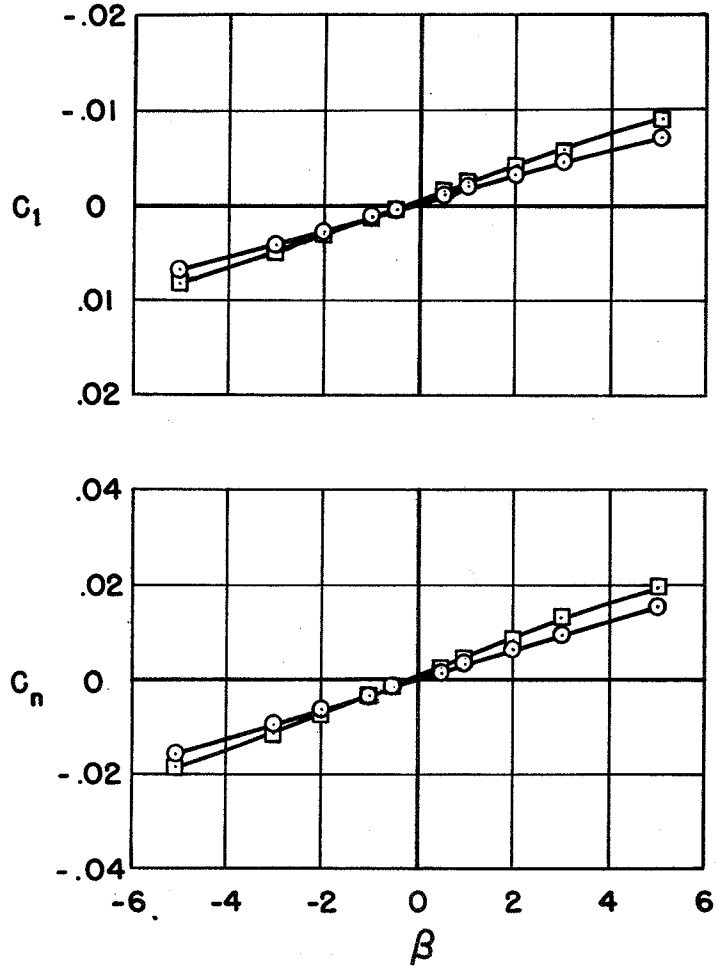
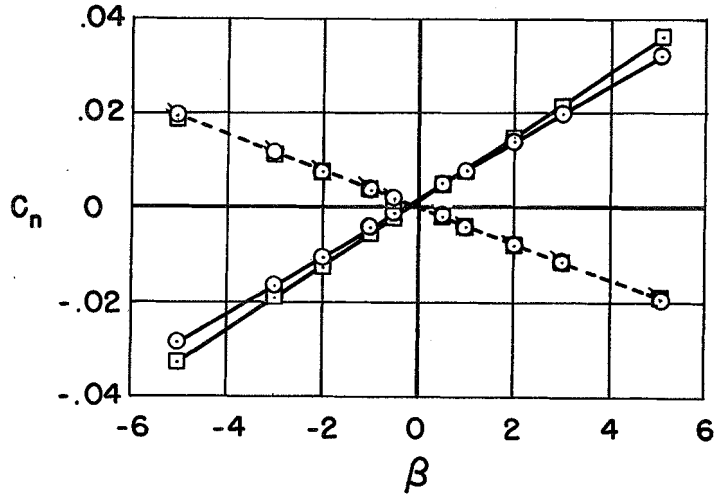(c) M = 1.90

Figure 4.- Concluded.
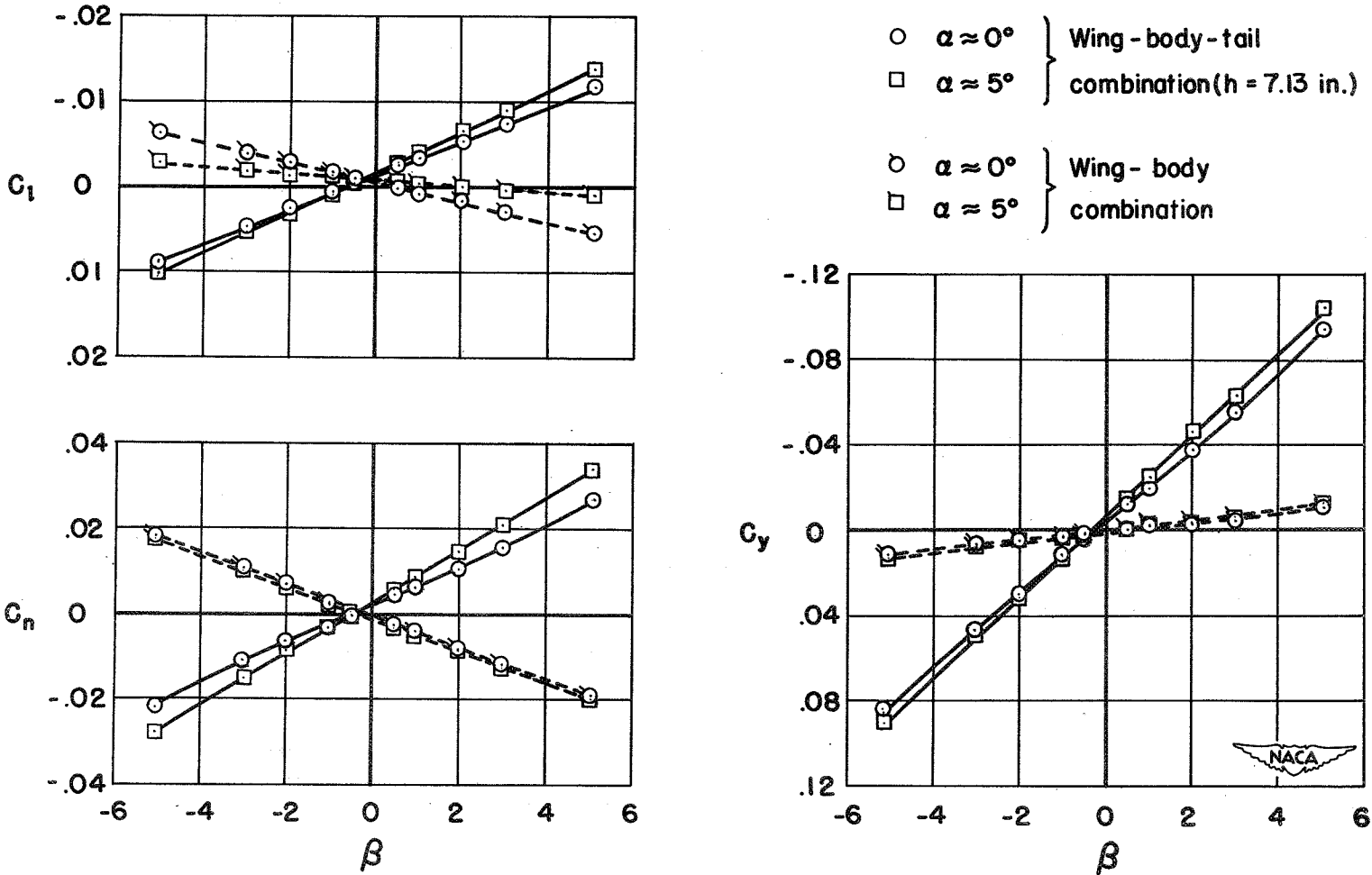
(a) M = 0.90

Figure 5.- Effect of angle of attack on the variation with sideslip angle of the rolling-moment, yawing moment, and cross-wind-force coefficients for a model of a fighter airplane; $\Gamma = -10°$.
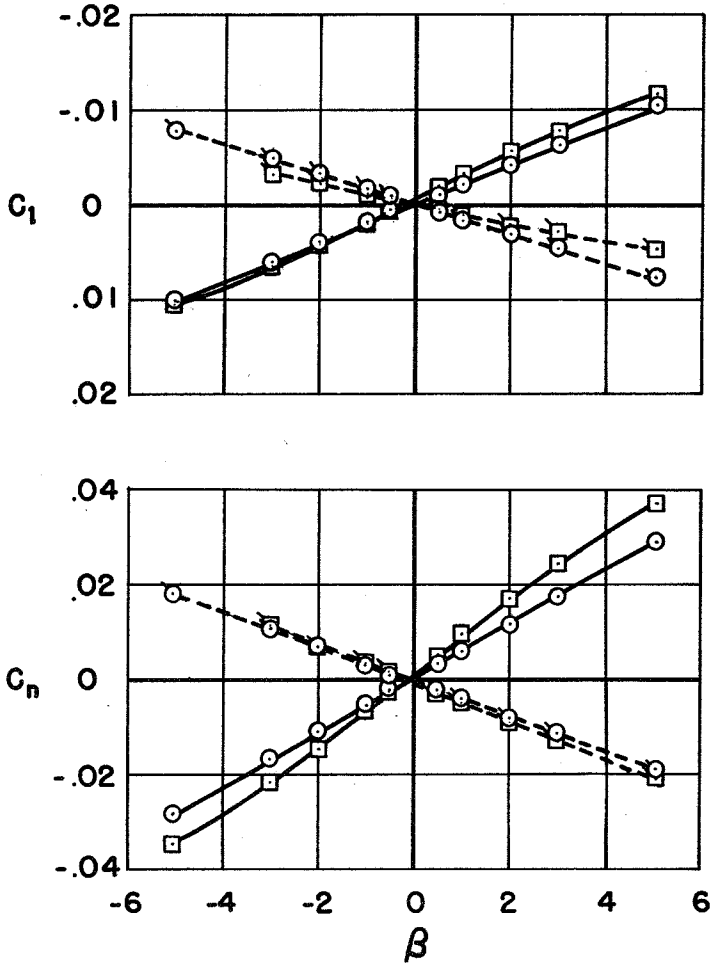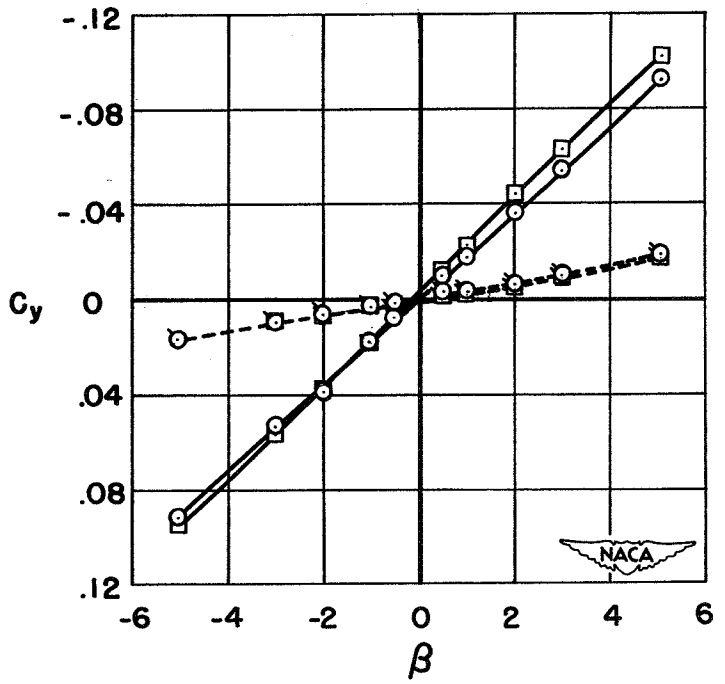
(b) $M = 1.45$

Figure 5.- Continued.
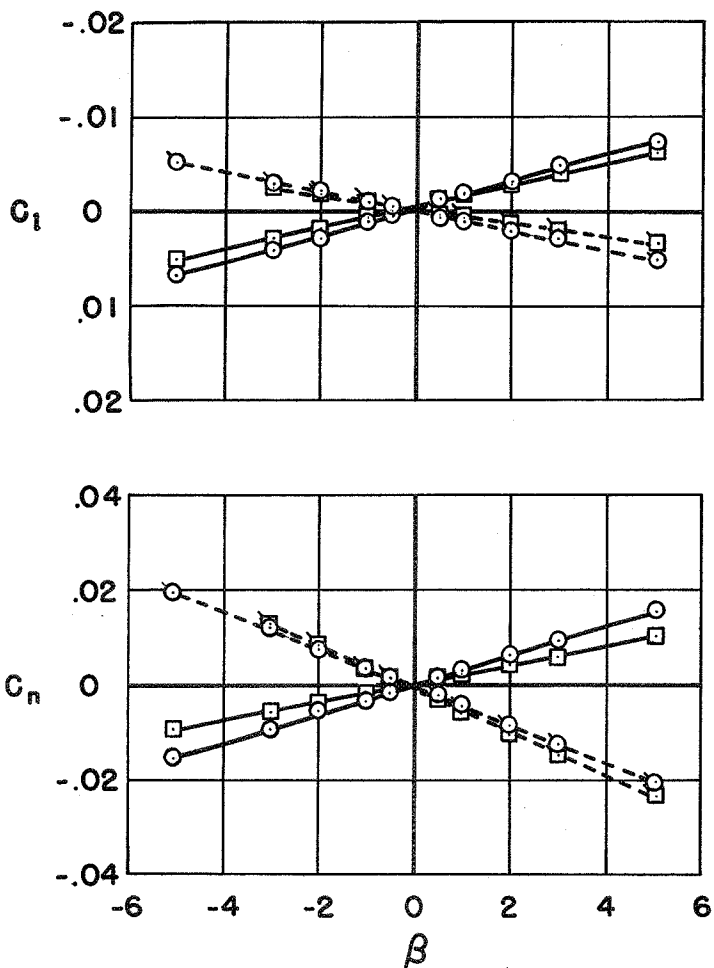
(c) M = 1.90

Figure 5.- Concluded.
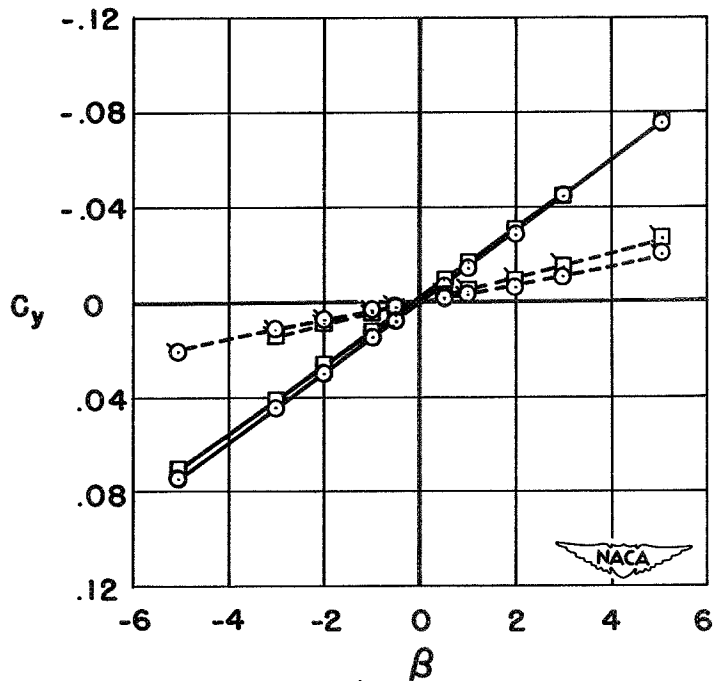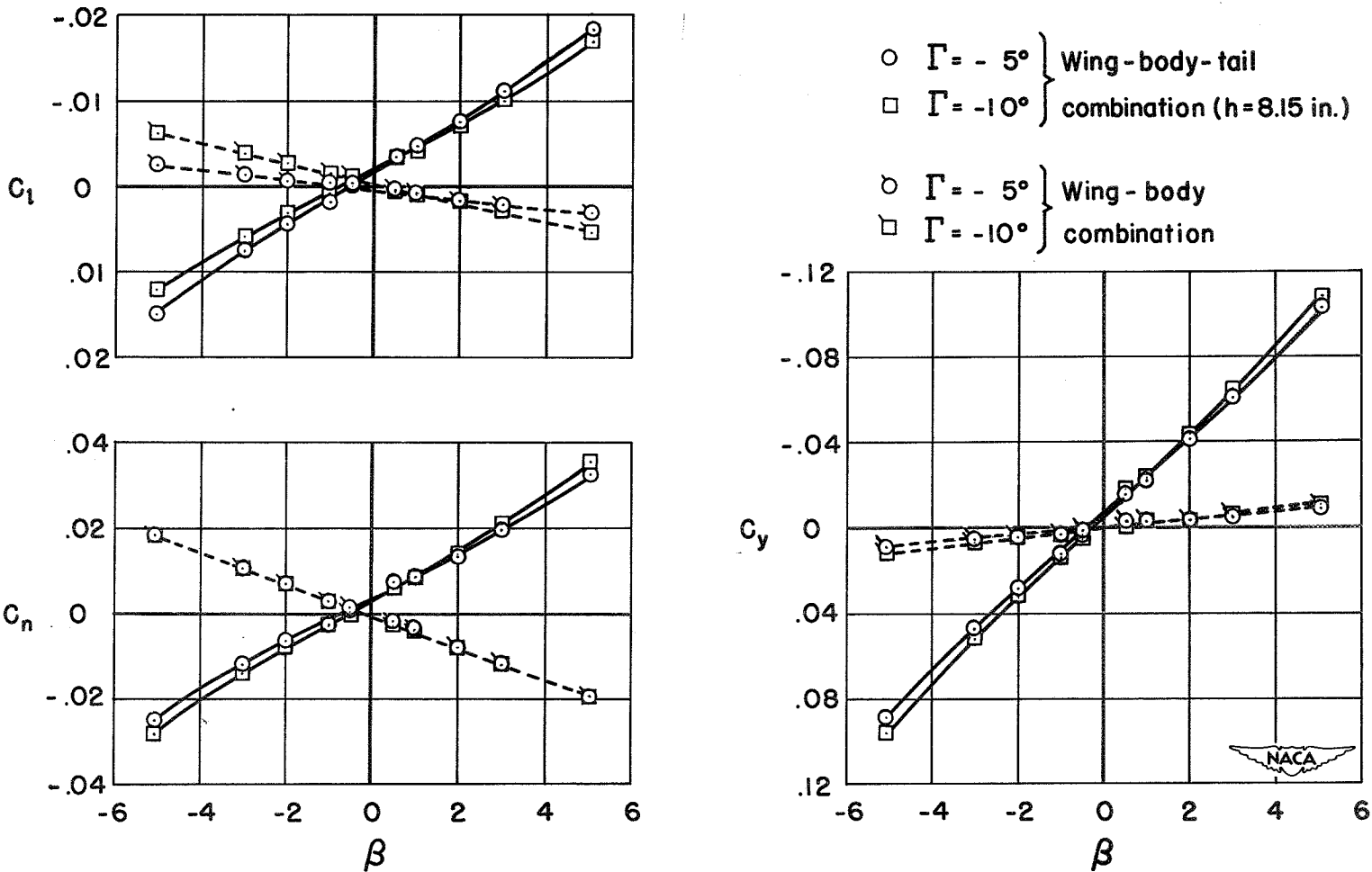
(a) M = 0.90

Figure 6.- Effect of wing dihedral on the variation with sideslip angle of the rolling-moment, yawing-moment, and cross-wind-force coefficients for a model of a fighter airplane; $\alpha \approx 0^{\circ}$.
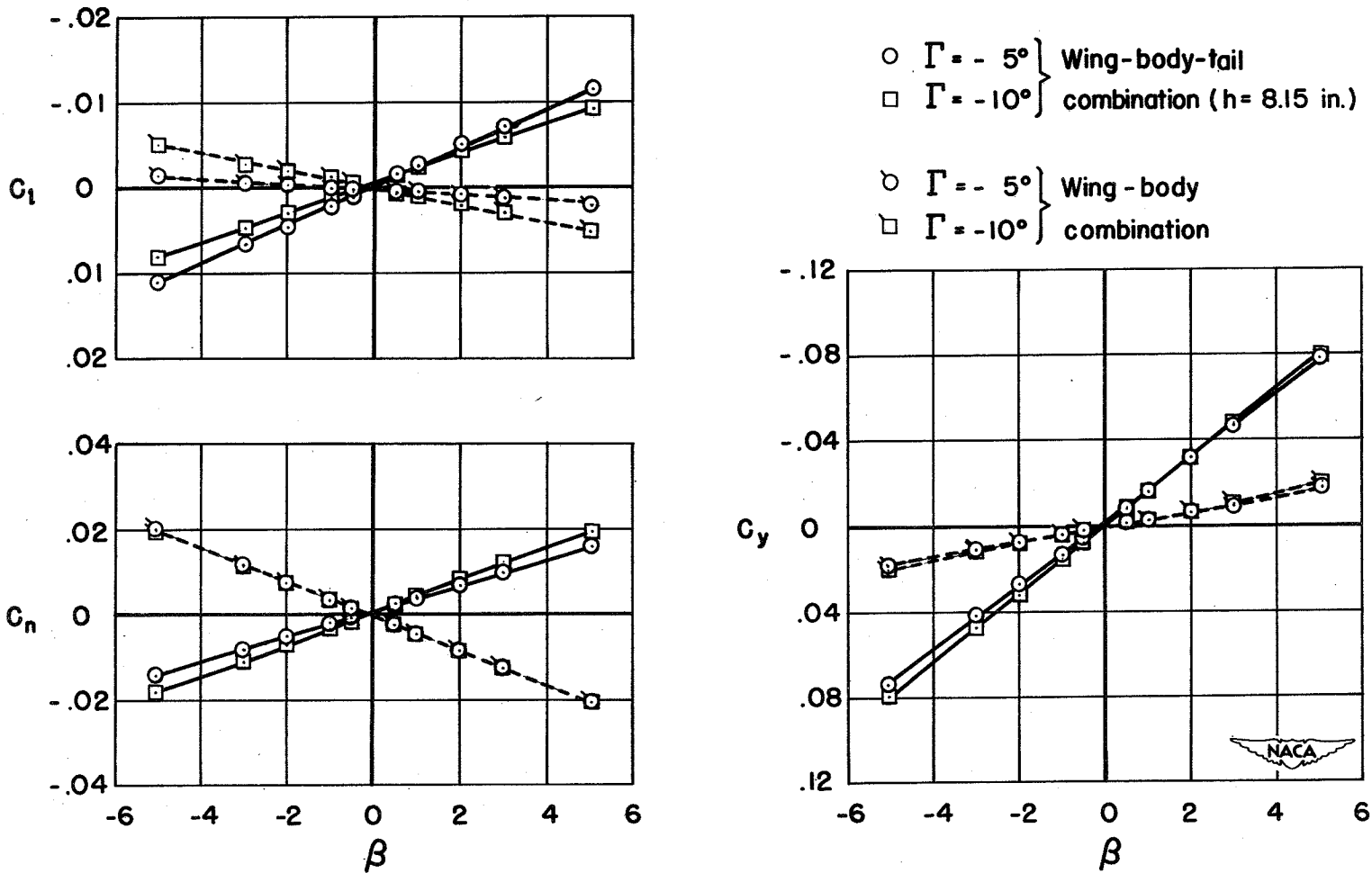
(b) M = 1.45

Figure 6.- Continued.

(c) M = 1.90

Figure 6.- Concluded.